photonics

MDPI

Communication

Time-Division Multiplexed Optical Covert Communication System Based on Gain-Switched Optical Pulses

Dong Liu, Yongliang Yin, Mingyu Cui, Zhanqi Liu and Huatao Zhu *

College of Information and Communication, National University of Defense Technology, Wuhan 430010, China
* Correspondence:zhuhuatao19@nudt.edu.cn

Abstract: In optical covert communication systems based on gain-switched distributed feedback semiconductor lasers, the trade-off between the modulation frequency and the spectral imperceptibility limits the bit rate of the secure channel. To improve the system performance in terms of the bit rate and covertness, optical time-division multiplexing is introduced to optical covert communication for the first time. The optical time-division multiplexed covert channel can work under both multiple-user and single-user conditions. The optical time-division multiplexed covert communication system is demonstrated via a system simulation. The results show that the covertness is enhanced by the optical time-division multiplexing in the spectral domain. The receiver sensitivity of the multiple-user condition is lower than the single-user one.

Keywords: semiconductor lasers; system performance; optical covert transmission; gain switching

1. Introduction

Photonic-layer secure communication safeguards against adversarial detection in the optical domain by employing a range of security technologies, including optical chaos [1–5], optical code division multiplexing [6–8], quantum noise randomized ciphers [9–12], optical frequency hopping [13–15], quantum key distribution [16,17], and optical covert communication (OCC) [18–23]. OCC requires a higher level of security than merely protecting the content from unauthorized access through encryption, and the security requirement is imperceptibility for optical covert communication.

To ensure the imperceptibility of a system, the signal output from the transmitter should be noise-like in the temporal and spectral domains. An amplified spontaneous emission (ASE) laser [24,25], a distributed feedback (DFB) semiconductor laser [26,27], an external cavity laser [28,29], or a mode-locked laser [30] can be used as carriers of the stealth signal after optical signal processing.

In addition to imperceptibility, there is a growing demand for increased capacity in optical covert communication systems due to the rising volume of information and data. Coherent lasers, such as DFB lasers and mode-locked lasers, show advantages from a capacity point of view. To further improve the capacity, a simple way is to enhance the modulation frequency. However, in DFB laser-based optical covert communication systems, an increase in the modulation frequency leads to an enhancement of the tone-to-noise ratio and a decrease in the concealment [31]. Additionally, the mode-locked lasers have a comb-shaped spectrum, which is a disadvantage for imperceptibility. Then, as a common method to improve capacity, multiplexing may be an option. A wavelength-division multiplex-based scheme has been demonstrated for OCC based on ASE [32], and it can also be applied in OCC based on a broadband coherent source, such as a super-continuum [27]. However, the wavelength resources that can be used by a stealth user are limited in a public network.

For the covertness or undetectability, in this paper, an optical time-division multiplexing method is proposed for an OCC system. The waveform and spectrum of the optical pulses generated by a DFB laser are analyzed. The optical covert signal undergoes optical

Citation: Liu, D.; Yin, Y.; Cui, M.; Liu, Z.; Zhu, H. Time-Division Multiplexed Optical Covert Communication System Based on Gain-Switched Optical Pulses. *Photonics* **2024**, *11*, 376. https://doi.org/10.3390/photonics11040376

Received: 3 February 2024
Revised: 4 April 2024
Accepted: 13 April 2024
Published: 17 April 2024

time-division multiplexing, optical encoding, and time spreading before being sent to the public channel. With different modulation frequencies at the DFB laser, the modulation parameters are optimized to achieve a proper performance. An optical covert communication system over four wavelength-division multiplexed optical public channels is set up in the system simulation.

2. Optical Time-Division Multiplexing Optical Covert Signal

A schematic diagram of optical time-division multiplexing optical covert signal generation is shown in Figure 1a. The total time slot of the optical time-division multiplexing optical stealth signal is m. The original signal in the covert channel is divided into several subsequence by the time-slot number, and the data subsequences are sent to different slots bit by bit. Thus, the data sequence achieves a serial-to-parallel transformation. A local oscillator activates a DFB laser to perform gain-switching on it. The gain-switched optical pulses have a period of T. Mach–Zehnder modulators with different time delays are modulated by the serial-to-parallel transformed signals. The time-division multiplexed signals are then combined using an optical coupler and forwarded to an all-optical encoder for time spreading to transform them into a noise-like signal. Another structure of optical time-division multiplexing optical covert signal generation is shown in Figure 1b. The gain-switched optical pulses are time-division multiplexed by time-delay lines and combined by an optical coupler. Then, the multiplexed signals are sent to the all-optical encoder. In an all-optical encoder, the gain-switched optical pulse is divided in the frequency domain by a wavelength-division multiplexer into different parts, each with a different time delay. Thus, the gain-switched optical pulses are encoded in both the frequency and time domains. The encoded signal is further spread in the time domain through a dispersive fiber after the optical encoder. Thus, the optical time-division multiplexed signal is processed to be a noise-like signal, and can be stealth-sent under optical noise in an optical network.

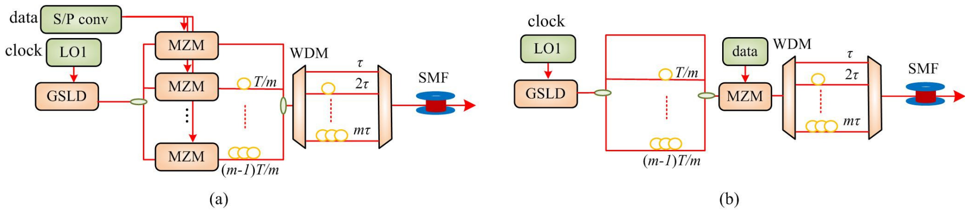

Figure 1. The generation of an optical time-division multiplexed optical covert signal, (**a**) multiple-user; (**b**) single-user. LO, local oscillator; MZM, Mach–Zehnder modulator; GSLD, gain-switched laser diode; WDM, wavelength division multiplexing.

In the gain-switching of a DFB laser, the interaction between photons and carriers in the DFB laser can be modeled by the rate equations [33–35]. The dynamics of the carrier density $N(t)$ and complex electric field $E(t)$ in the DFB laser can be expressed as follows:

$$\begin{aligned} \frac{dE(t)}{dt} &= \frac{v_g a(N(t)-N_t)\Gamma E(t)}{2[1+\varepsilon E^2(t)]} - \frac{E(t)}{2\tau_p} + \frac{\Gamma\beta B N^2(t)}{2E(t)} + F_E \\ \frac{dN(t)}{dt} &= \frac{I(t)}{eV} - \frac{v_g a(N(t)-N_0)}{1+\varepsilon E^2(t)} E^2(t) - \frac{N(t)}{\tau_n} + F_N \end{aligned} \quad (1)$$

where the names and values of the parameters are listed in Table 1. The signal output from the local oscillator is $I(t)$, which is a time-varying injection current and contains the bias current I_b and sinusoidally varying current I_m. The Langevin noise sources F_E and F_N take into account spontaneous emission and spontaneous carrier recombination.

For a DFB laser gain-switched by a 10 GHz electrical signal, the waveform and spectrum are shown in Figures 2a and c, respectively. I_b is 0.2 A and I_m is 0.2 A. The spectra of the gain-switched optical pulses are optical frequency combs. For a DFB laser gain-switched by a 2.5 GHz electrical signal, the waveform and spectrum of the optical time-division multiplexed signal are shown in Figure 2b,d. I_b is 0.08 A and I_m is 0.2 A. The optical time-division multiplexed signals have the same bit rate as 10 Gbps optical pulses, and the spectrum is continuum and wideband.

Table 1. Some parameter definitions and values used in the simulations.

Parameter	Value
Confinement factor (Γ)	0.3
Linear material gain coefficient (a)	3.3×10^{-20} m^2
Spontaneous emission rate (β)	1×10^{-4}
Group velocity (v_g)	7.5×10^7 ms^{-1}
Electron charge (e)	1.6×10^{-19} C
Volume of the active region (V)	1.8×10^{-16} m^3
Carrier density at transparency (N_t)	1.5×10^{24} m^{-3}
Nonlinear gain compact factor (ε)	3×10^{-23} m^3
Photon lifetime (τ_p)	3×10^{-12} s
Carrier life time at threshold (τ_n)	2.1×10^{-9} s
Bimolecular recombination coefficient (B)	1.0×10^{-16} m^{3}s^{-1}

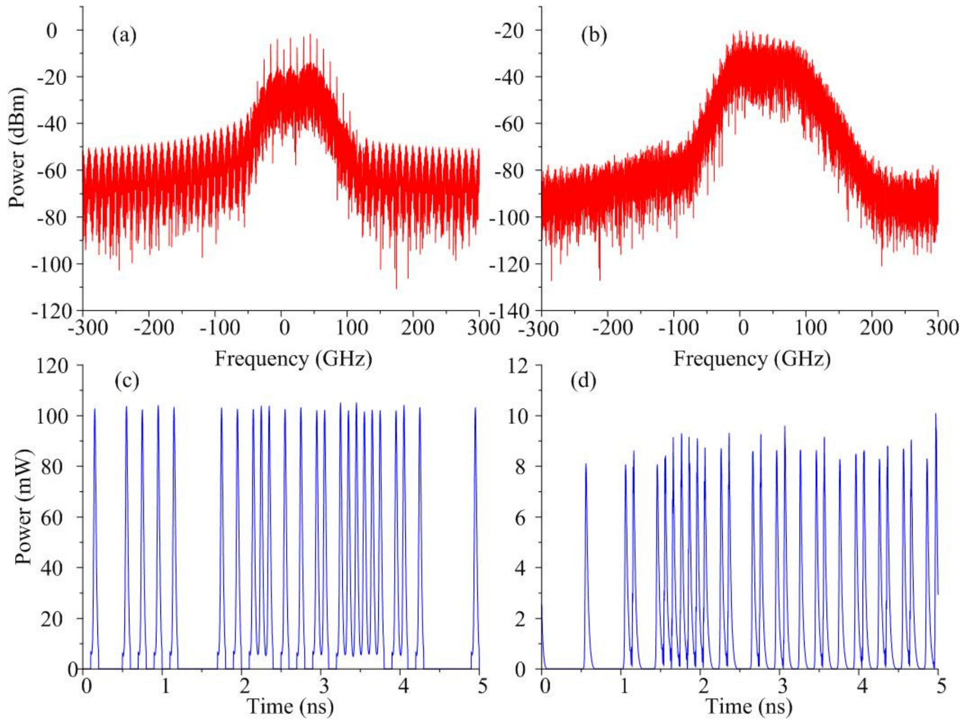

Figure 2. The waveform and spectrum of the optical time-division multiplexed signal. (**a**,**c**) 10 Gbps signal; (**b**,**d**) 4 time-division multiplexed 2.5 Gbps signal.

3. Optical Covert Communication System

A schematic diagram for the proposed time-division multiplexed OCC system based on gain-switched optical pulses is shown in Figure 3. The public channel consists of four signals with center frequencies of 192.81, 193.02, 193.22, and 193.42 THz. The public optical signals are modulated by a non-return to zero (NRZ) signal with bit rate of 10 Gbps. The optical covert signal is sent to the public channel through an optical coupler, which is followed by a 50 km single-mode fiber (SMF) span. The optical covert transmitter has the same structure as that in Figure 1a. In the public receiver, the public signals are directly detected after passing through a dispersion-compensation fiber and a de-multiplexer. For the optical covert channel, the public signals are suppressed by an optical filter and then amplified by an EDFA. The residual dispersion is compensated by a fiber span with a dispersion of −332 ps/nm. The time-compressed signal is then decoded by the decoder and then de-multiplexed in the time domain by an electro-absorption modulator. The signal is restored through P/S conversion before the BER tester.

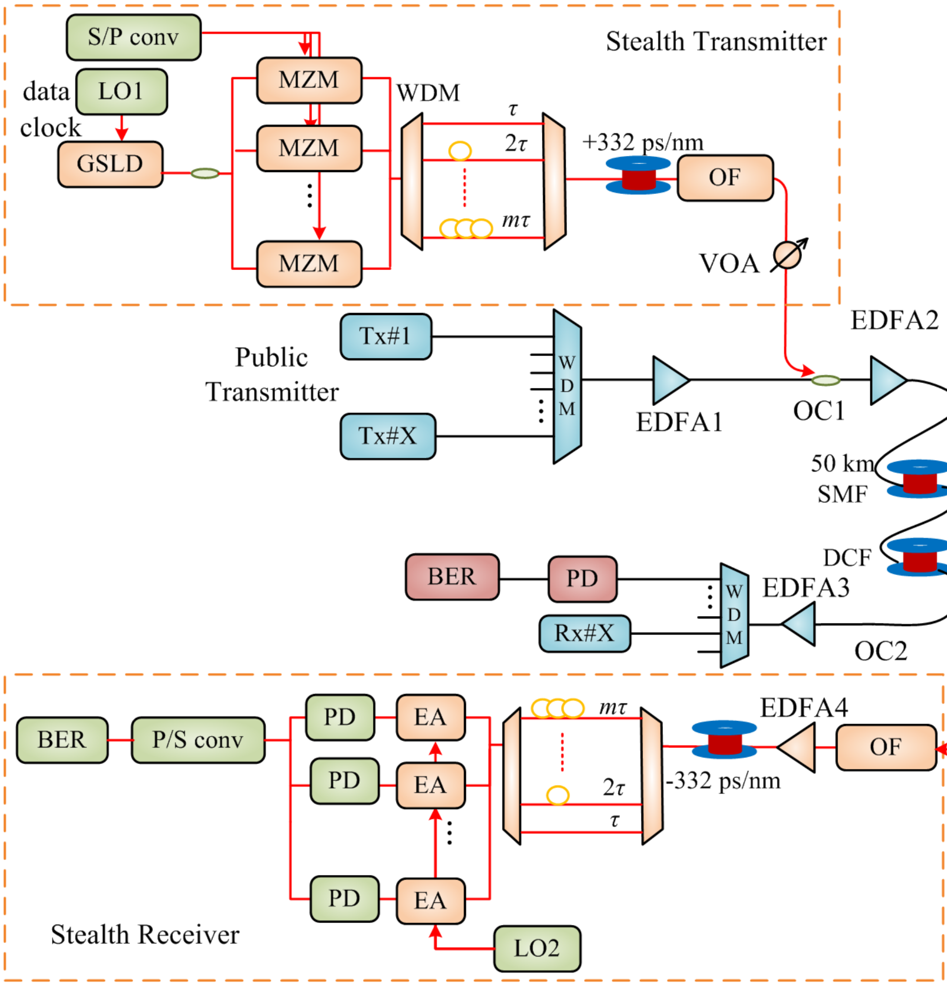

Figure 3. Schematic diagram of the proposed optical time-division multiplexing optical covert communication system. LO, local oscillator; S/P, serial-to-parallel; MZM, Mach–Zehnder modulator; GSLD, gain-switched laser diode; WDM, wavelength-division multiplexing; OF, optical filter; VOA, variable optical attenuator; EDFA, Erbium-doped fiber amplifier; DCF, dispersion-compensating fiber; BER, bit-error rate tester; EA, electro-absorption modulator.

4. Simulation Results and Discussion

4.1. Multiple Users

To quantitatively analyze the influence of optical time-division multiplexing on the system performance, the BER performance of the optical covert channel was studied and shown in Figure 4. The covert signals were modulated by a 2.5 GHz electrical signal and then multiplexed in 4-fold by time delay lines and an optical coupler. As can be seen, the covert signal can be transmitted error-free over a 50 km public transmission link, in which the bias current is 0.08 A and the modulation current is 0.2 A. Due to the different performance of the electro-absorption modulators in the time domain, the receiver sensitivity varies from one time slot to another.

The BER curves versus the different received powers of the public channels are shown in Figure 5. As can be seen, the public channels have different receiver sensitivities. When comparing the BER curves with the ASE noise and with the covert signal, the power penalty is smaller than 0.3 dB. Therefore, the optical time-division multiplexed covert signals have a minimal impact on the public channel.

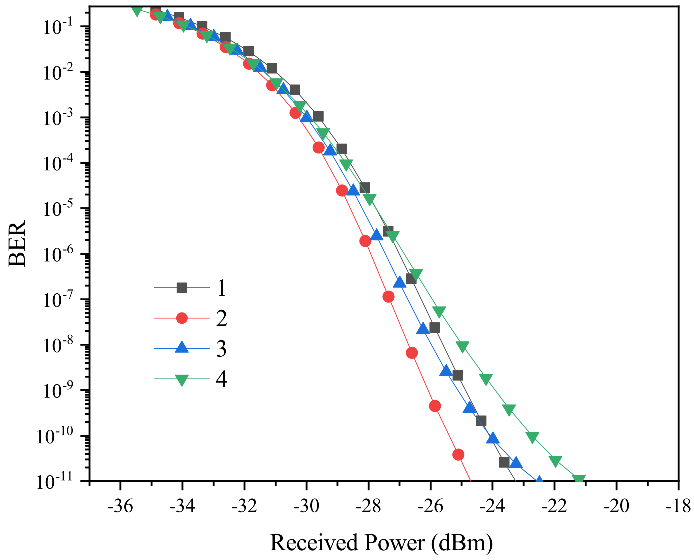

Figure 4. The BER curves of the covert channel.

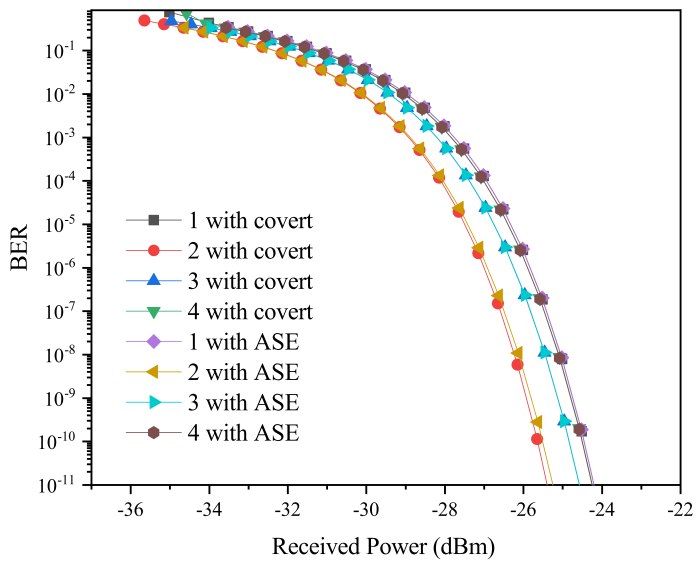

Figure 5. The BER curves of the public channel.

The eye diagrams of the optical covert channel are shown in Figure 6. As can be seen, the bit rate is 10 Gbps after optical time-division multiplexing. Then, the optical pulses are mixed in with each other after optical encoding; however, the envelope is clear. After time spreading, the optical pulses are noise-like in the time domain, as can be seen in Figure 6c. Then, the noise-like signal can be transmitted under the ASE noise in the optical network.

Combined with the optical covert signal, the spectra of the public channel are shown in Figure 7. Comparing the spectrum of the public channel with the ASE noise and with the optical covert signal, there is little difference. With the ASE noise introduced by the optical amplifier, the covert signal can be hidden with a lower optical signal-to-noise ratio.

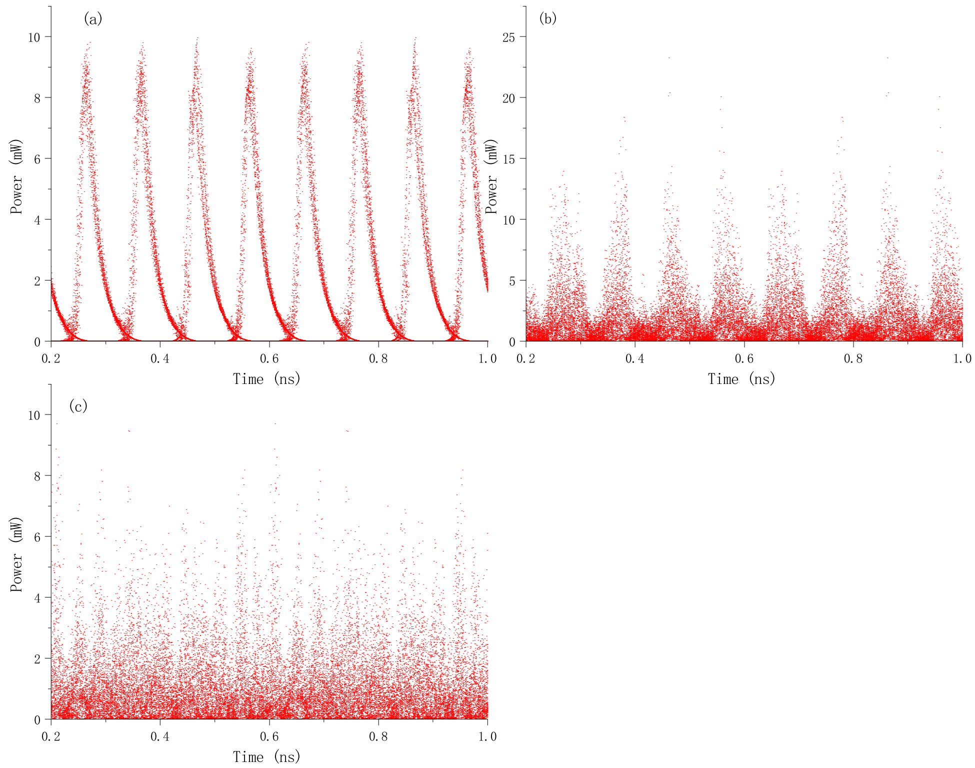

Figure 6. Eye diagrams of the covert channel: (**a**) the multiplexed optical pulses; (**b**) the encoded signal; and (**c**) the spread signal.

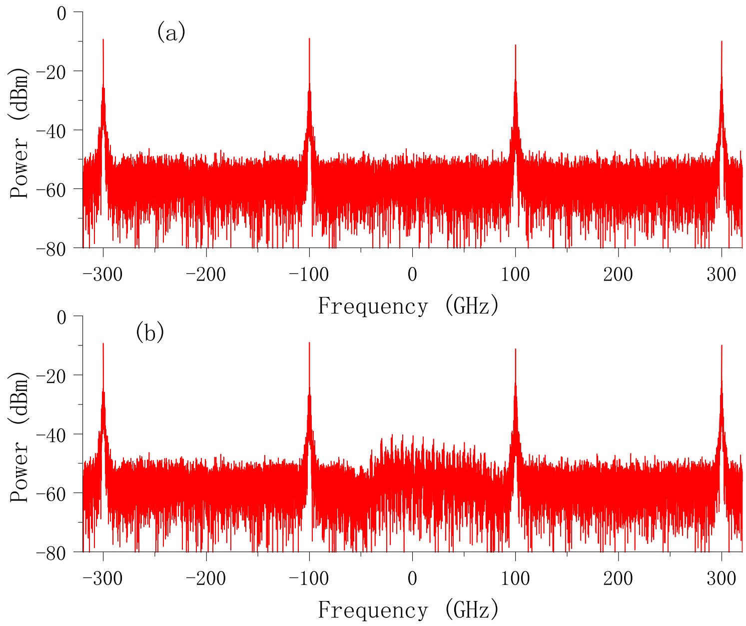

Figure 7. The spectrum of the public channel: (**a**) with the ASE noise and (**b**) with the optical covert signal.

Eye diagrams of the public channel with the ASE noise and with optical covert signal are shown in Figure 8. The center frequency of the public signal is 193.02 THz. The two eye diagrams show no difference in the time domain. Therefore, the optical covert channel is hidden in the public channel and has no impact on the public signal.

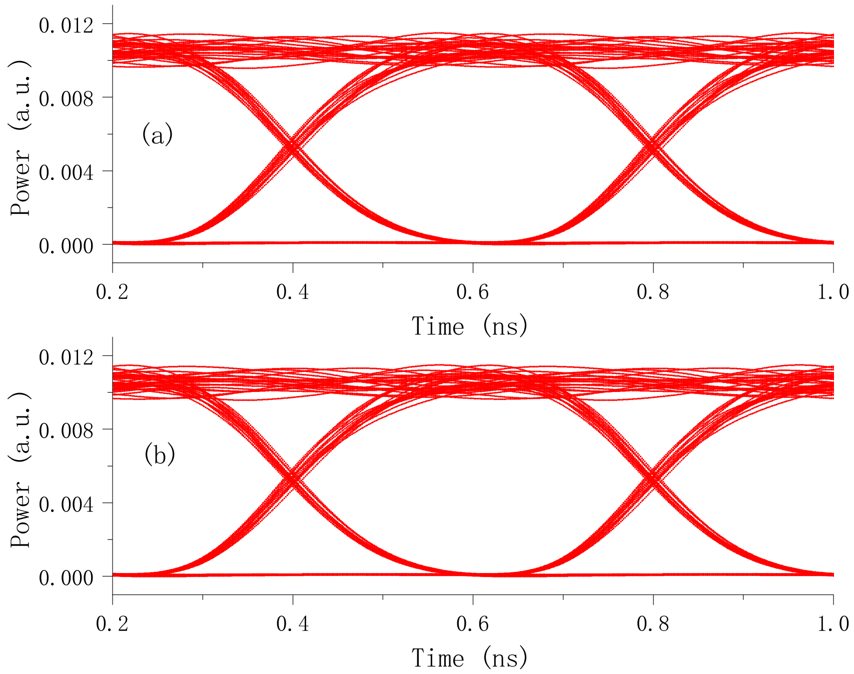

Figure 8. Eye diagram of the public channel: (**a**) with the ASE noise; and (**b**) with the optical covert signal.

4.2. Single User

After being optical time-division multiplexed, the covert signal was modulated by a 10 Gbps signal for a single user. The BER curve of the 10 Gbps optical covert signal is shown in Figure 9. The optical covert channel can be transmitted error-free. In addition, the receiver sensitivity of the single-user covert channel is larger than that of the multiple-user covert channel.

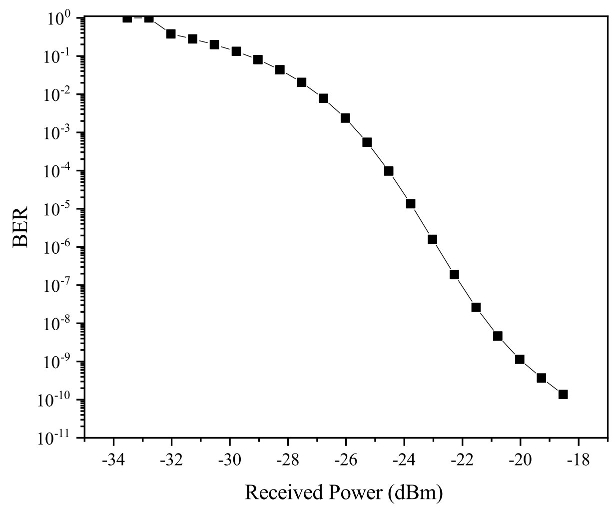

Figure 9. The BER curve of the covert channel.

The BER curves versus the different received powers of the public channels are shown in Figure 10. Compared with Figure 5, the public channels have similar receiver sensitivities. Furthermore, when comparing the BER curves with the ASE and with the covert signal, it is observed that there is a minor power penalty for the public channel when a single-user optical covert channel is present. Hence, the architecture employed for optical time-division multiplexing has a negligible effect on the performance of the public channel.

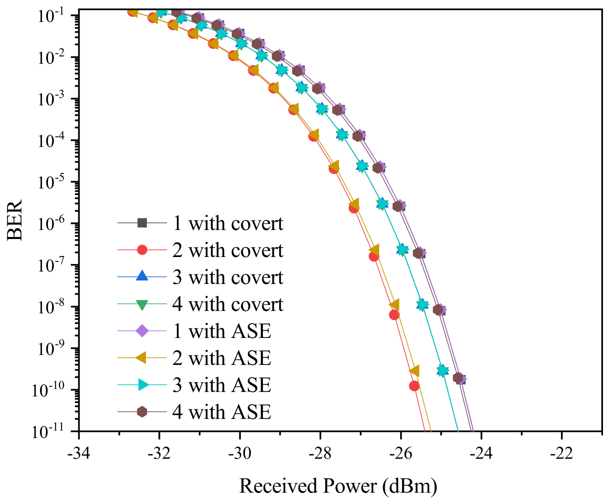

Figure 10. The BER curves of the public channel.

5. Discussions and Conclusions

The optical time-division multiplexed covert channel for multiple users has a low receiver sensitivity; however, an electro-absorption modulator or another de-multiplexing device is necessary in the receiver. Thus, for point-to-point communication, optical time-division multiplexed covert channels are suitable for modulating a single message so that the receiver does not have to be de-multiplexed and the concealment performance is similarly improved.

Considering the multiplexing approach, the available bandwidth is limited for signal transmission through optical network equipment. Optical time-division multiplexing is a good choice for increasing the number of users and capacity.

In summary, in order to improve the system performance of optical covert communication, optical time-division multiplexing is introduced in this paper. System simulations have validated the effectiveness of the optical time-division multiplexing in optical covert communication systems. The simulation results show that the covert channel can be transmitted error-free after being optical time-division multiplexed. The structure of the optical time-division multiplexer has no influence on the public channel, but has an impact on the covert channel. Hence, this work provides a novel solution to enhance the bit rate and covertness of optical covert communication.

Author Contributions: Conceptualization, H.Z.; methodology, D.L., Y.Y., M.C., Z.L. and H.Z.; validation, D.L. and Z.L.; formal analysis, Y.Y. and M.C.; investigation, D.L., Y.Y., M.C., Z.L. and H.Z. All authors have read and agreed to the published version of the manuscript.

Funding: This work was supported in part by the National Natural Science Foundation of China under Grant No. 61901480, 62301569.

Institutional Review Board Statement: Not applicable.

Informed Consent Statement: Not applicable.

Data Availability Statement: The data presented in this study are available on request from the corresponding author. The data are not publicly available due to the data also forms part of an ongoing study.

Conflicts of Interest: The authors declare no conflict of interest.

References

1. Argyris, A.; Syvridis, D.; Larger, L.; Annovazzi-Lodi, V.; Colet, P.; Fischer, I.; Garcia-Ojalvo, J.; Mirasso, C.R.; Pesquera, L.; Shore, K.A. Chaos-based communications at high bit rates using commercial fibre-optic links. *Nature* **2005**, *438*, 343–346. [CrossRef]
2. Pal, B.; Baruah, S.; Dikshit, B. Synchronization of complexity enhanced chaos in semiconductor lasers. *Phys. Scr.* **2024**, *99*, 15525. [CrossRef]
3. Zhang, Y.; Xu, M.; Pu, M.; Zhou, M.; Ding, J.; Chen, S.; Qiu, K.; Jiang, N.; Luo, X. Simultaneously enhancing capacity and security in free-space optical chaotic communication utilizing orbital angular momentum. *Photonics Res.* **2023**, *11*, 2185–2193. [CrossRef]
4. Deng, Z.; Gao, X.; An, Y.; Wang, A.; Fu, S.; Wang, Y.; Yuwen, Q.; Gao, Z. High-speed secure key distribution based on interference spectrum-shift keying with signal mutual modulation in commonly driven chaos synchronization. *Opt. Express* **2023**, *31*, 42449–42463. [CrossRef]
5. Li, N.; Nguimdo, R.M.; Locquet, A.; Citrin, D.S. Enhancing optical-feedback-induced chaotic dynamics in semiconductor ring lasers via optical injection. *Nonlinear Dyn.* **2018**, *92*, 315–324. [CrossRef]
6. Abd El-Mottaleb, S.A.; Singh, M.; Atieh, A.; Aly, M.H. Performance evaluation of a UOWC system based on the FRS/OCDMA code for different types of Jerlov waters. *Appl. Opt.* **2024**, *63*, 762–771. [CrossRef]
7. Ji, J.; Wu, B.; Zhang, J.; Xu, M.; Wang, K. Design and Investigation of 10 Gb/s FSO Wiretap Channel Using OCDMA Time-Diversity Reception. *IEEE Photonics J.* **2020**, *12*, 7903212. [CrossRef]
8. Ahmed, M.S.; Glesk, I. Management of OCDMA Auto-Correlation Width by Chirp Manipulation Using SOA. *IEEE Photonics Technol. Lett.* **2018**, *30*, 785–788. [CrossRef]
9. Li, Y.; Li, Y.; Zhu, K.; Wei, S.; Zhang, M.; Zhao, Y.; Zhang, J. Integrating key generation and distribution with the quantum noise stream cipher system without compromising the transmission performance. *Opt. Lett.* **2023**, *48*, 6500–6503. [CrossRef]
10. Yoshida, M.; Kan, T.; Kasai, K.; Hirooka, T.; Nakazawa, M. 10 Tbit/s QAM Quantum Noise Stream Cipher Coherent Transmission Over 160 Km. *J. Light. Technol.* **2021**, *39*, 1056–1063. [CrossRef]
11. Tanizawa, K.; Futami, F. IF-Over-Fiber Transmission of OFDM Quantum-Noise Randomized PSK Cipher for Physical Layer Encryption of Wireless Signals. *J. Light. Technol.* **2022**, *40*, 1698–1704. [CrossRef]
12. Zhu, K.; Wei, S.; Li, Y.; Li, Y.; Wang, Y.; Zhao, Y.; Zhang, J. Quantum Noise Stream Cipher Scheme With Triangular Quadrature Amplitude Modulation and Secret Probabilistic Shaping. *J. Light. Technol.* **2024**, *42*, 1423–1433. [CrossRef]
13. Ban, D.C.; Huang, Q.C.; Chen, Y.F.; Qi, Y.C.; Chen, W.; Zhu, N.H. A Novel Optical Frequency-Hopping Scheme Based on a Flexible Structure for Secure Optical Communications. *IEEE Photonics J.* **2019**, *11*, 1–7. [CrossRef]
14. Darabi, E.; Keshavarz, H.; Monteiro, P. A Novel Reconfigurable Nonlinear Cascaded MZM Mixer, Amplitude Shift Key Modulator (ASK), Frequency Hopping and Phase Shifter. *Photonics* **2023**, *10*, 916. [CrossRef]
15. Wang, J.; Jin, Y.; Xie, Z.; Chen, Y.; Liu, Y.; Zhu, N. Secure FSO communication based on optical frequency-hopping technology using delay interferometers. *Opt. Commun.* **2024**, *550*, 129939. [CrossRef]
16. Klicnik, O.; Munster, P.; Horvath, T. Multiplexing Quantum and Classical Channels of a Quantum Key Distribution (QKD) System by Using the Attenuation Method. *Photonics* **2023**, *10*, 1265. [CrossRef]
17. Zheng, Z.; Guo, X.; Lin, F.; Wang, Y.; Wang, Y.; Guo, Y. Parallel CV-QRNG with Strict Entropy Evaluation. *Photonics* **2023**, *10*, 786. [CrossRef]
18. Zhu, H.; Liu, Z.; Chen, S.; Xu, X.; Li, F. Optical stealth communication based on quantum noise stream ciphered amplified spontaneous emission light. *Opt. Express* **2023**, *31*, 3595. [CrossRef]
19. Yen, C.T.; Huang, J.F.; Zhang, W.Z. Hiding Stealth Optical CDMA Signals in Public BPSK Channels for Optical Wireless Communication. *Appl. Sci.* **2018**, *8*, 1731. [CrossRef]
20. Zhu, H.; Liu, Z.; Xiang, P.; Chen, S.; Li, F.; Xu, X. Quantum noise ciphered optical stealth communication based on equivalent spectral encoding. *Opt. Express* **2022**, *30*, 38128. [CrossRef]
21. Laka, P.; Maksymiuk, L. Steganographic transmission in optical networks with the use of direct spread spectrum technique. *Secur. Commun. Netw.* **2016**, *9*, 771–780. [CrossRef]
22. Liu, Z.; Zhu, H.; Zhang, X.; Chen, S.; Xu, X.; Li, F. Subnoise optical covert communication based on amplified spontaneous emission light. *Opt. Express* **2023**, *31*, 40261. [CrossRef]
23. Senkans, U.; Bobrovs, V.; Ivanovs, G.; Spolitis, S. Research of hybrid WDM-PON data transmission system with embedded ASE-powered stealth channels for steganography applications. *Opt. Fiber Technol.* **2020**, *58*, 102300. [CrossRef]
24. Wu, B.; Wang, Z.; Tian, Y.; Fok, M.P.; Shastri, B.J.; Kanoff, D.R.; Prucnal, P.R. Optical steganography based on amplified spontaneous emission noise. *Opt. Express* **2013**, *21*, 2065–2071. [CrossRef] [PubMed]
25. Huang, C.; Ma, P.Y.; Shastri, B.J.; Mittal, P.; Prucnal, P.R. Robustness of Optical Steganographic Communication Under Coherent Detection Attack. *IEEE Photonics Technol. Lett.* **2019**, *31*, 327–330. [CrossRef]
26. Hong, X.; Wang, D.; Xu, L.; He, S. Demonstration of optical steganography transmission using temporal phase coded optical signals with spectral notch filtering. *Opt. Express* **2010**, *18*, 12415–12420. [CrossRef]
27. Zhu, H.; Wang, R.; Pu, T.; Fang, T.; Xiang, P.; Zheng, J.; Chen, D. Optical stealth transmission based on super-continuum generation in highly nonlinear fiber over WDM network. *Opt. Lett.* **2015**, *40*, 2561–2563. [CrossRef]
28. Wohlgemuth, E.; Yoffe, Y.; Goki, P.N.; Imran, M.; Fresi, F.; Poti, L.; Sadot, D. Demonstration of Stealthy and Encrypted Optical Transmission Below Adjacent 50 GHz DWDM Channels. *IEEE Photonics Technol. Lett.* **2020**, *32*, 581–584. [CrossRef]

29. Wohlgemuth, E.; Yoffe, Y.; Yeminy, T.; Zalevsky, Z.; Sadot, D. Demonstration of coherent stealthy and encrypted transmission for data center interconnection. *Opt. Express* **2018**, *26*, 7638–7645. [CrossRef]
30. Fok, M.P.; Wang, Z.; Deng, Y.; Prucnal, P.R. Optical Layer Security in Fiber-Optic Networks. *IEEE Trans. Inf. Forensics Secur.* **2011**, *6*, 725–736. [CrossRef]
31. Wang, X.; Mou, W.; Zhu, H. Effect of Laser Parameters on Optical Stealth Transmission System Performance. *Sensors* **2021**, *21*, 5358. [CrossRef] [PubMed]
32. Wu, B.; Tait, A.N.; Chang, M.P.; Prucnal, P.R. WDM optical steganography based on amplified spontaneous emission noise. *Opt. Lett.* **2014**, *39*, 5925–5928. [CrossRef] [PubMed]
33. Schunk, N.; Petermann, K. Noise analysis of injection-locked semiconductor injection lasers. *IEEE J. Quantum Electron.* **1986**, *22*, 642–650. [CrossRef]
34. Fatadin, I.; Ives, D.; Wicks, M. Numerical Simulation of Intensity and Phase Noise From Extracted Parameters for CW DFB Lasers. *IEEE J. Quantum Electron.* **2006**, *42*, 934–941. [CrossRef]
35. Cartledge, J.C.; Srinivasan, R.C. Extraction of DFB laser rate equation parameters for system simulation purposes. *J. Light. Technol.* **1997**, *15*, 852–860. [CrossRef]